Supporting information

New Class of "Electro-acid/base" Induced Reversible Methyl Ketone Colour Switches

Yumo Zhang,[a] Minjie Li,[,a] Wen Li,[a] Zhiyuan Huang,[a] Shaoyin Zhu,[a] Bing Yang,[a] Xiao-Chun Wang,[b] and Sean Xiao-An Zhang[*,a]*

[a] *State Key Laboratory of Supramolecular Structure and Materials, College of Chemistry, Jilin University, Changchun, Jilin 130012 (China)*

[b] *Institute of Atomic and Molecular Physics, Jilin University, Changchun, Jilin 130012 (China)*

Table of Contents

1. Experimental details

2. Characterization of mechanism for M1

3. Absorption spectra and cyclic voltammogram of M2 - M7

electric field and base.

Figure S14. Absorption spectra and cyclic voltammogram of **M5** stimulated by electric field and base.

Figure S15. Absorption spectra of **M6** and nitrobenzene mixture solution stimulated by electric field and base.

Figure S16. Absorption spectra of **M7** and nitrobenzene mixture solution stimulated by electric field and base.

Figure S17. Schematic depiction of an adiabatic intermolecular proton transfer reaction.

Figure S18. Illustration of in-situ spectroelectrochemical characterization.

Figure S19. Illustration of the ITO cells of liquid film.

Figure S20. Illustration of the ITO cells of PMMA film.

4. ^{1}H NMR and ^{13}C NMR of M1 - M8

1. Experimental details

1.1 Materials

Fluorene, 2-(4-nitrophenyl)acetic acid and 2-(2-nitrophenyl)acetic acid were purchased from Aldrich. 2-(4-(trifluoromethyl)phenyl)acetic acid, 2-(4-(methylsulfonyl)phenyl)acetic acid, ethylene glycol, benzene, anisole, ferrocene, and tetrabutylammonium hexafluorophosphate (TBAPF$_6$) were purchased from Aladdin. TBAPF$_6$ was recrystallized three times from ethanol and dried under vacuum at 50 °C. Acetonitrile was distilled from CaH$_2$ under nitrogen prior to use. Other chemicals were used as received except for those mentioned.

1.2 Characterization of Synthesis

2-(4-nitrophenyl)-1-phenylethanone (M1). A pale yellow solid, yield (85 %). ^{1}H NMR (300 MHz, CDCl$_3$): δ=8.21 (d, *J* = 8.8 Hz, 2H), 8.02 (d, *J* = 7.1 Hz, 2H), 7.62 (t, *J* = 7.4 Hz, 1H), 7.51 (t, *J* = 7.7 Hz, 2H), 7.44 (d, *J* = 8.8 Hz, 2H), 4.42 (s, 2H). ^{13}C NMR (75 MHz, CDCl$_3$): δ=195.91, 146.99, 142.01, 136.09, 133.65, 130.58, 128.80, 128.35, 123.64, 44.85. LC-HRMS: calcd for C$_{14}$H$_{12}$NO$_3$ 242.0812, found 242.0805. m.p.: 141.3-142.0 °C.

1-(4-methoxyphenyl)-2-(4-nitrophenyl)ethanone (M2). A pale yellow solid, yield (86 %). ^{1}H NMR (300 MHz, CDCl$_3$): δ=8.20 (d, *J* = 8.8 Hz, 2H), 7.99 (d, *J* = 9.0 Hz, 2H), 7.43 (d, *J* = 8.8 Hz, 2H), 6.96 (d, *J* = 9.0 Hz, 2H), 4.36 (s, 2H), 3.89 (s, 3H). ^{13}C NMR (75 MHz, CDCl$_3$): δ=194.59, 164.08, 146.99, 142.63, 130.92, 130.68, 129.30, 123.81, 114.14, 55.67, 44.77. LC-HRMS: calcd for C$_{15}$H$_{14}$NO$_4$ 272.0917, found 272.0913. m.p.: 112.2-113.0 °C.

1-(9,9-dihexyl-9H-fluoren-2-yl)-2-(4-nitrophenyl)ethanone (M3). A pale yellow solid, yield (80 %). ^{1}H NMR (300 MHz, CDCl$_3$): δ = 8.22 (d, *J*=8.3, 2H), 8.01 (d, *J*=8.0, 1H), 7.98 (s, 1H), 7.78 (d, *J*=7.8, 2H), 7.48 (d, *J*=8.4, 2H), 7.38 (s, 3H), 4.47 (s, 2H), 1.99 (t, *J*=8.2, 4H), 1.15–0.93 (m, 12H), 0.75 (t, *J*=7.2, 6H), 0.56 (m, 4H). ^{13}C NMR (75 MHz, CDCl$_3$): δ=195.91, 152.11, 151.41, 147.08, 146.82, 142.62, 139.57, 134.78, 130.75, 128.81, 128.21, 127.21, 123.77, 123.20, 122.81, 120.94, 119.78, 55.42, 45.24, 40.25, 31.54, 29.68, 23.82, 22.61, 14.05. LC-HRMS: m/z calc. for C$_{33}$H$_{44}$NO$_3$ 498.3003, found 498.2996. m.p.: 85.6-86.6°C.

2-(4-nitrophenyl)-1-p-tolylethanone (M4). A pale yellow solid, yield (68 %). ^{1}H NMR (300 MHz, CDCl$_3$): δ=8.19 (d, *J* = 8.8 Hz, 2H), 7.90 (d, *J* = 8.3 Hz, 2H), 7.42 (d, *J* = 8.8 Hz, 2H), 7.29 (d, *J* = 7.9 Hz, 2H), 4.38 (s, 2H), 2.42 (s, 3H). ^{13}C NMR (75 MHz, CDCl$_3$): δ=195.71, 147.09, 144.79, 142.43, 133.80, 130.71, 129.64, 128.67, 123.78, 44.93, 21.78. LC-HRMS: calcd for C$_{15}$H$_{14}$NO$_3$ 256.0974, found 256.0968. m.p.: 111.8-112.2 °C.

1-(4-methoxyphenyl)-2-(2-nitrophenyl)ethanone (M5). A pale yellow solid, yield (85 %). ^{1}H NMR (300 MHz, CDCl$_3$): δ=8.14 (dd, *J* = 8.1, 1.3 Hz, 1H), 8.02 (d, *J* = 8.9 Hz, 2H), 7.61 (td, *J* = 7.5, 1.4 Hz, 1H), 7.52 – 7.42 (m, 1H), 7.35 (dd, *J* = 7.6, 1.4 Hz, 1H), 6.98 (d, *J* = 8.9 Hz, 2H), 4.69 (s, 2H), 3.89 (s, 3H). ^{13}C NMR (75 MHz, CDCl$_3$, ppm): δ=193.72, 163.71, 149.08, 133.56, 133.34, 130.84, 130.46, 129.42, 128.17, 125.06, 113.81, 55.45, 43.61. LC-HRMS: calcd for C$_{15}$H$_{14}$NO$_4$ 272.0917, found 272.0915. m.p.: 114.3-115.5 °C.

1-(4-methoxyphenyl)-2-(4-(methylsulfonyl)phenyl)ethanone (M6). A pale yellow solid, yield (50 %). ^{1}H NMR (300 MHz, CDCl$_3$): δ=7.99 (d, J = 8.8 Hz, 2H), 7.18 (d, J = 8.5 Hz, 2H), 6.92 (d, J = 8.8 Hz, 2H), 6.86 (d, J = 8.7 Hz, 2H), 4.17 (s, 2H), 3.86 (s, 3H), 3.78 (s, 3H). ^{13}C NMR (75

MHz, CDCl$_3$): δ=194.90, 164.09, 141.48, 139.20, 130.97, 130.79, 129.34, 127.78, 114.17, 55.70, 44.90, 44.72. LC-HRMS: calcd for C$_{16}$H$_{17}$O$_4$S 305.0848, found 305.0842. m.p.: 175.5-176.2 °C.

**1-(4-methoxyphenyl)-2-(4-(trifluoromethyl)phenyl)ethanone (M7)** A pale yellow solid, yield (90 %). ^{1}H NMR (300 MHz, CDCl$_3$): δ=7.99 (d, J = 8.9 Hz, 2H), 7.58 (d, J = 8.2 Hz, 2H), 7.38 (d, J = 8.1 Hz, 2H), 6.95 (d, J = 8.9 Hz, 2H), 4.30 (s, 2H), 3.87 (s, 3H). ^{13}C NMR (75 MHz, CDCl$_3$): δ=194.89, 163.52, 138.71, 132.43, 131.29, 130.55, 129.62, 129.07, 128.80, 128.60, 128.17, 127.78, 125.73, 125.25, 125.20, 125.16, 125.10, 122.12, 114.47, 113.89, 113.65, 113.30, 113.09, 55.20, 44.47. LC-HRMS: calcd for C$_{16}$H$_{14}$F$_3$O$_2$ 295.0940, found 295.0941. m.p.: 137.0-137.8 °C.

2-methyl-2-(4-nitrophenyl)-1-phenylpropan-1-one (M9). To an ice-cooled solution of M1 (241 mg, 1 mmol) in dry THF (10 mL) under an argon atmosphere was added *t*-BuOK (280 mg, 2.5 mmol), and the solution was stirred at room temperature for 1.5 h. Then CH$_3$I (0.156 ml, 2.5 mmol) was added. The reaction mixture was stirred for a further 4 h. KI was then removed by filtration, and concentrated in vacuum. The product was separated by column chromatography using petroleum ether and ethyl acetate (v:v=20:1) as eluent. A pale yellow solid, yield (230 mg, 85%). ^{1}H NMR (300 MHz, CDCl$_3$): δ=8.22 (d, *J* = 8.9 Hz, 2H), 7.61 − 7.35 (m, 5H), 7.25 (t, *J* = 7.6 Hz, 2H), 1.66 (s, 6H) ^{13}C NMR (75 MHz, CDCl$_3$, ppm): δ=199.05, 148.61, 146.85, 135.79, 133.31, 128.68, 128.58, 124.06, 47.31, 19.25. LC-HRMS: calcd for C$_{12}$H$_{15}$NO$_3$ 270.1130, found 270.1128. m.p.: 85.1-86.2 °C.

2-(4-nitrobenzyl)-2-phenyl-1,3-dioxolane (M10). A mixture of ethylene glycol (0.28 ml, 5 mmol), p-toluene sulphonic acid (0.017 g, 0.1 mmol), **M1** (0.24 g, 1 mmol) and toluene (10 ml) was refluxed for 2 days using a Dean-Stark. After cooled, the solvent was removed by a rotary evaporator. The residue was dissolved in 200 ml of CH$_2$Cl$_2$, and washed with aqueous sodium carbonate. The combined organic layers were dried over MgSO$_4$, filtered and concentrated in vacuum. The product was separated by column chromatography using petroleum ether and ethyl acetate (v:v=10:1) as eluent. A pale yellow solid, yield (90 %). ^{1}H NMR (300 MHz, CDCl$_3$): δ=8.06 (d, *J* = 10.5 Hz, 2H), 7.52 − 7.12 (m, 7H), 3.96 − 3.57 (m, 4H), 3.26 (s, 2H). ^{13}C NMR (75 MHz, CDCl$_3$) δ =146.48, 143.51, 141.46, 131.36, 127.89, 127.85, 125.38, 122.48, 109.08, 64.46, 46.48. LC-HRMS: calcd for C$_{16}$H$_{16}$NO$_4$ 286.1079, found 286.1073. m.p.: 119.0-119.9 °C.

1,2-diphenylethanone (M11). A pale yellow solid, yield (95%). ^{1}H NMR (300 MHz, CDCl$_3$): δ=8.08 − 7.95 (m, 2H), 7.60 − 7.51 (m, 1H), 7.46 (tt, *J* = 6.7, 1.6 Hz, 2H), 7.37 − 7.21 (m, 5H), 4.29 (s, 2H). ^{13}C NMR (75 MHz, CDCl$_3$): δ=197.70, 136.70, 134.63, 133.23, 129.55, 128.75, 128.72, 128.69, 126.96, 45.58. LC-HRMS: calcd for C$_{14}$H$_{12}$O 196.0888, found 196.0894. m.p.: 87.3-88.1 °C.

2. Characterization of mechanism for M1
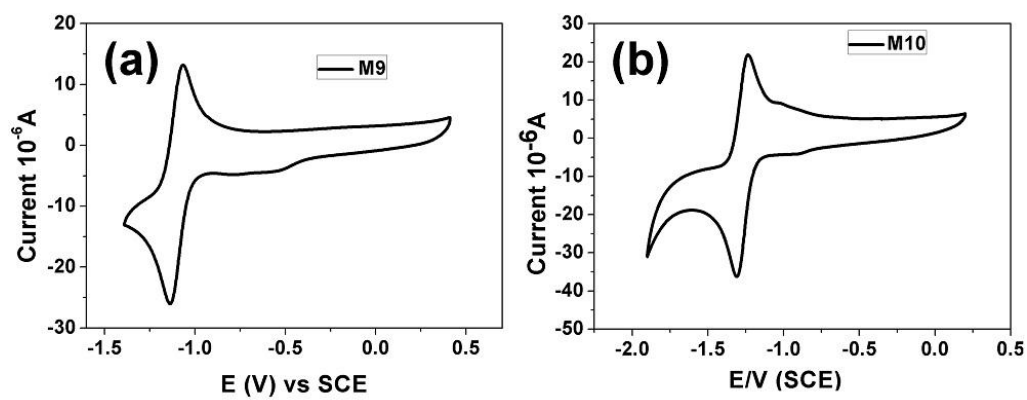
Figure S1. Cyclic voltammograms (CV) of **M9** (1.0×10^{-3} M) (a) and **M10** (1.0×10^{-3} M) (b) in acetonitrile containing $TBAPF_6$ (0.1 M). Scan rate: 100 mV/s.
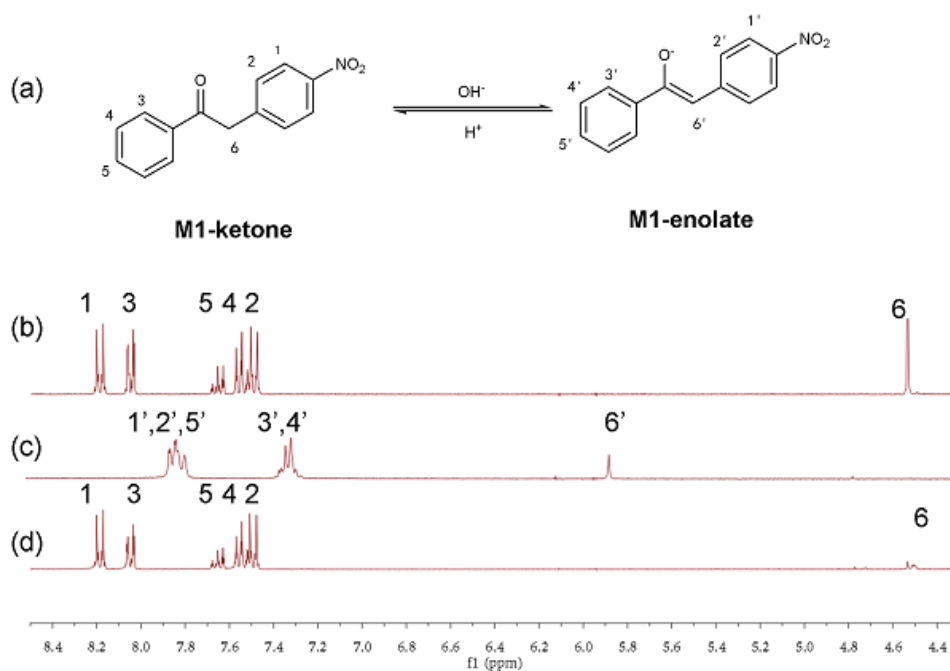
Figure S2. ^{1}H NMR spectra of (a) **M1-ketone** in CD_3CN; (b) **M1-enolate** obtained by adding 7 equiv of potassium tert-butoxide to **M1-ketone**; (c) **M1-ketone**, obtained by adding 7 equiv of CF_3COOD to **M1-enolate**. Due to deuterium exchange with CD_3CN solvent, the intensity for proton 6 decreases, and another broad peak appeared at 4.51 ppm assigned for the chemical shift of the proton 6 with one H deuterated.
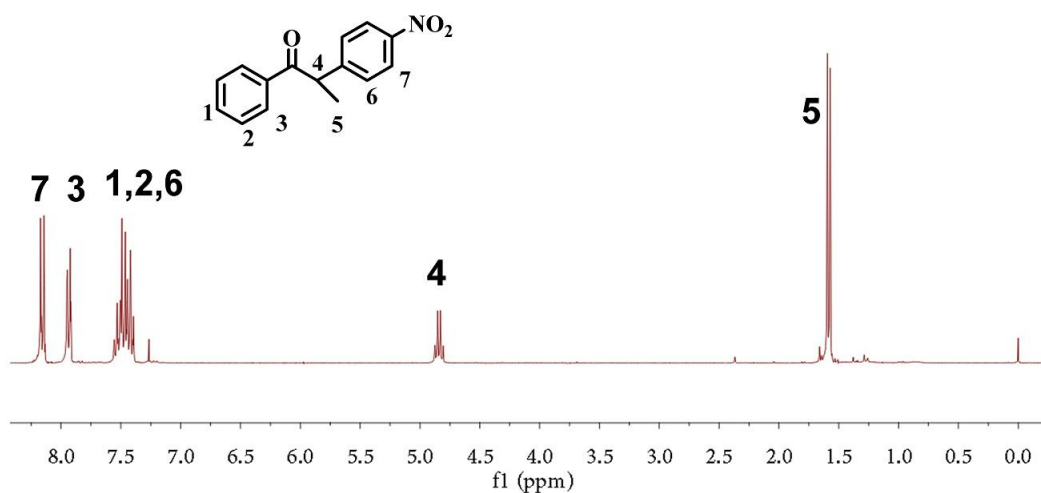
Figure S3. ^{1}H NMR spectra of M8 in CDCl$_3$. **M8** was separated from the electrolyte of cathode of H -type electrolytic cell by column chromatography using petroleum ether and ethyl acetate (v:v=20:1) as eluent. ^{1}H NMR (300 MHz, CDCl$_3$) δ=8.22 – 8.11 (d, J = 8.8 Hz, 2H), 7.98 – 7.89 (d, J = 7.1 Hz, 2H), 7.57 – 7.34 (m, 5H), 4.84 (q, J = 6.9 Hz, 1H), 1.58 (d, J = 6.9 Hz, 3H).
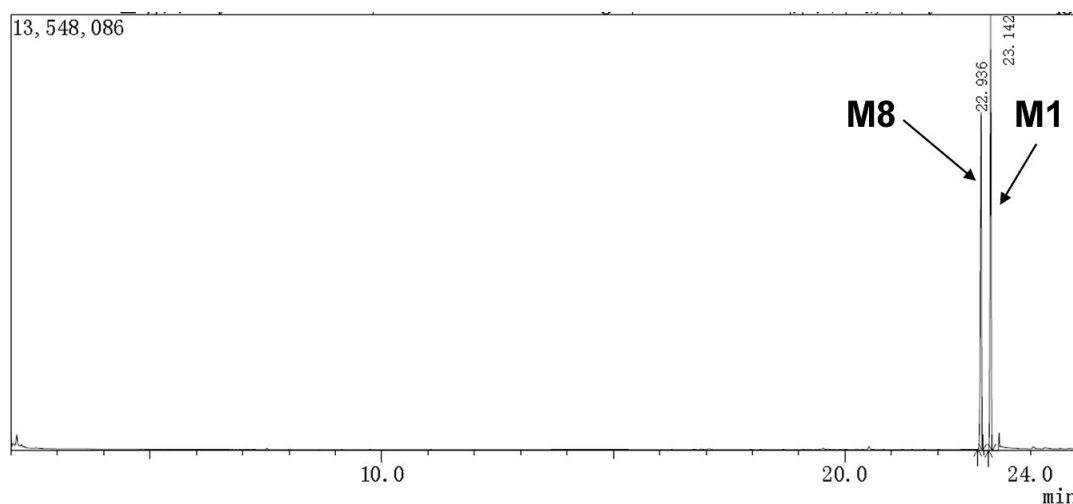
Figure S4. GC analysis of the sample of cathode of H-type electrolytic cell. This electrolytic cell was used for separating the electrolytic liquid from the anode and the cathode. The solvent of cathode was removed by a rotary evaporator. The residue was dissolved in 10 ml of ethyl acetate, and washed with aqueous. The combined organic layers afforded the sample.
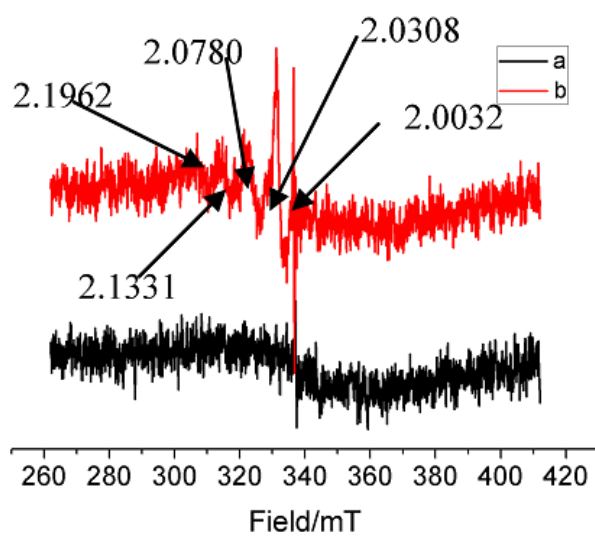
Figure S5. EPR spectrum of **M1** (1.0×10^{-3} M) in acetonitrile containing TBAPF$_6$ (0.1 M) (curve a), under -1.18 V (curve b).
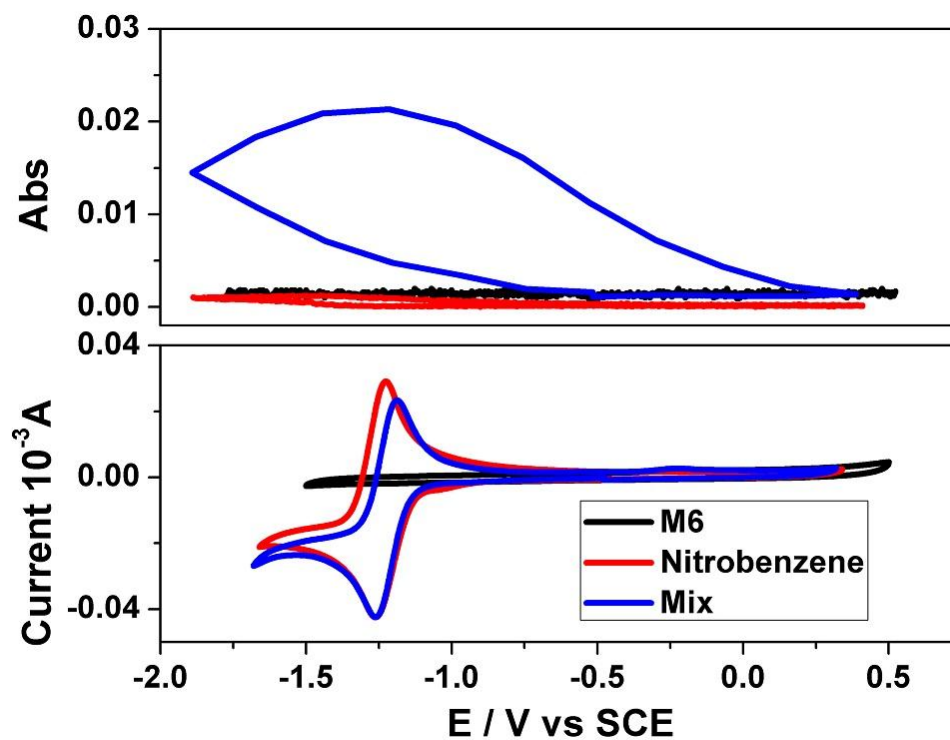
Figure S6 Changes in absorption at 416 nm (top) and cyclic voltammograms (bottom) of M6 (1.0×10^{-3} M), nitrobenzene (1.0×10^{-3} M) and M7/nitrobenzene (1.0×10^{-3} M/1.0×10^{-3} M), in acetonitrile with 0.1 M TBAPF6 on glassy carbon electrode (d = 3 mm). Scan rate: 50 mV/s.
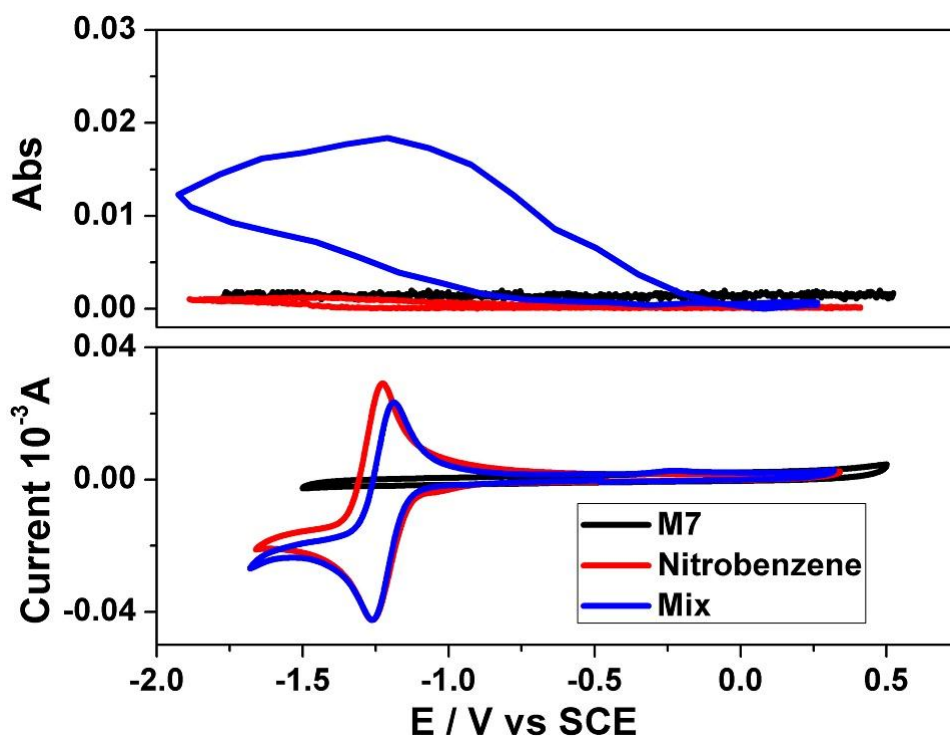
Figure S7 Changes in absorption at 389 nm (top) and cyclic voltammograms (bottom) of M7 (1.0×10^{-3} M), nitrobenzene (1.0×10^{-3} M) and M7/nitrobenzene (1.0×10^{-3} M/1.0×10^{-3} M), in acetonitrile with 0.1 M TBAPF6 on glassy carbon electrode (d = 3 mm). Scan rate: 50 mV/s.
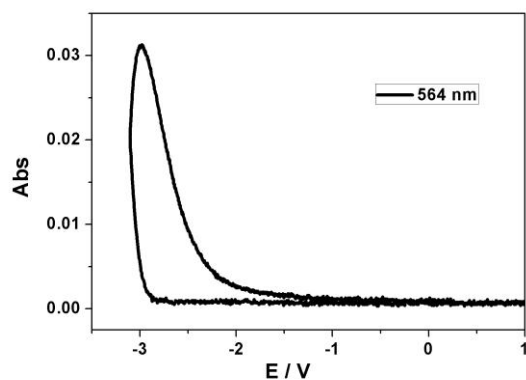
Figure S8 Cyclic voltammogram (CV) of the liquid device of **M1**. From this CV, we choose -3.0 V as turn-on voltage for the liquid device and 2.0 V as turn-off voltage.
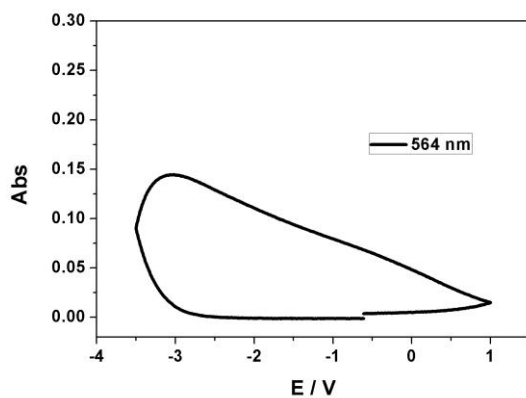
Figure S9 Cyclic voltammogram (CV) of the solid device of **M1**. From this CV, we choose -3.5 V as turn-on voltage for the solid device and 2.0 V as turn-off voltage.
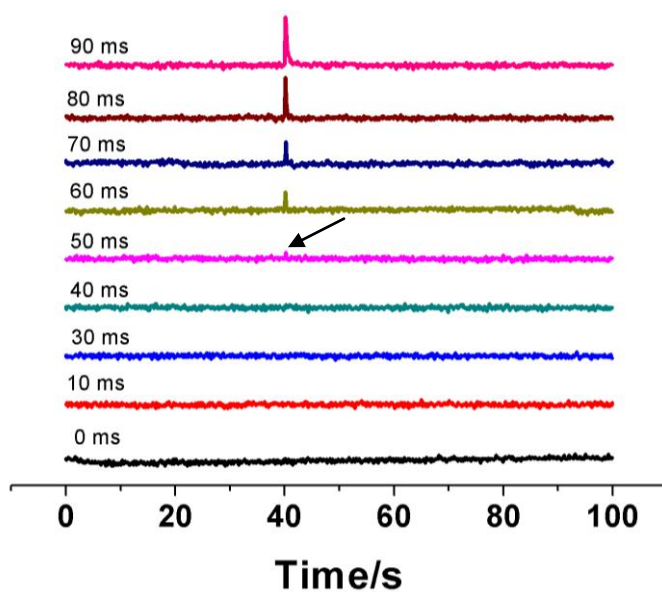
Figure S10. Variation of absorbance of **M1** at 564 nm with time. Impulse voltages of -3.0 V were applied at 40 s and the impulse times were from 0 ms to 90 ms. An absorbance change is observed at the impulse of 50 ms as labeled with arrow).

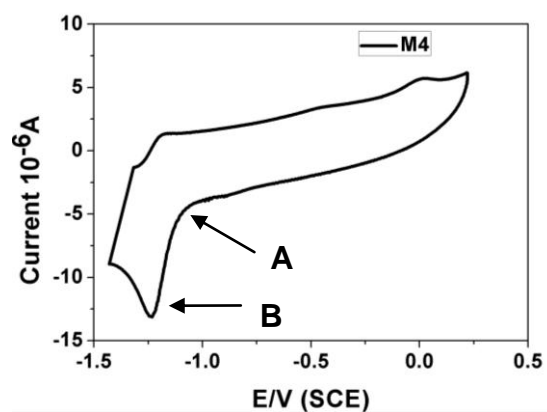## 3. Absorption spectra and cyclic voltammogram of M2-M7
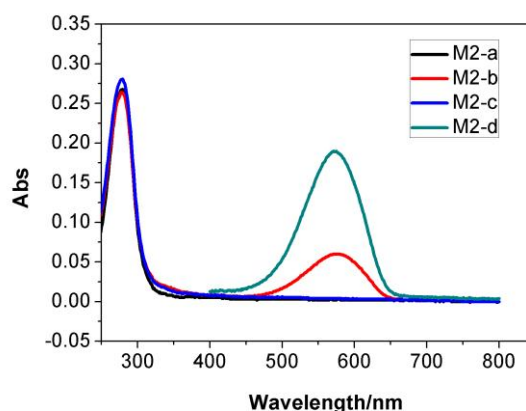
Figure S11 (a). Absorption spectra of **M2** (1.0×10^{-5} M) in acetonitrile (black curve), treated with potassium tert-butoxide (red curve), then neutralized with CH_3COOH (blue curve). Absorption spectrum of **M2** (1.0×10^{-3} M) in acetonitrile containing $TBAPF_6$ (0.1 M) under -3.0 V bias in ITO device (green curve).
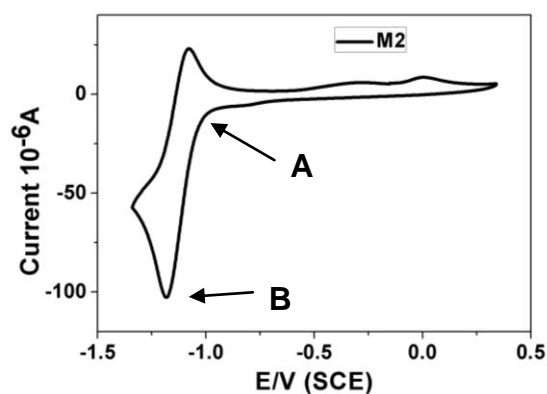
Figure S11 (b). Cyclic voltammogram (CV) of **M2** (1.0×10^{-3} M) in acetonitrile containing $TBAPF_6$ (0.1 M). Scan rate: 100 mV/s. The switch threshold of **M2** is labeled with arrow A and the oxidation peak of carbonyl group is labeled with arrow B.
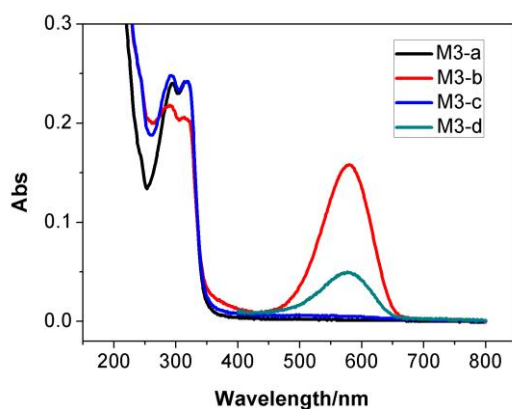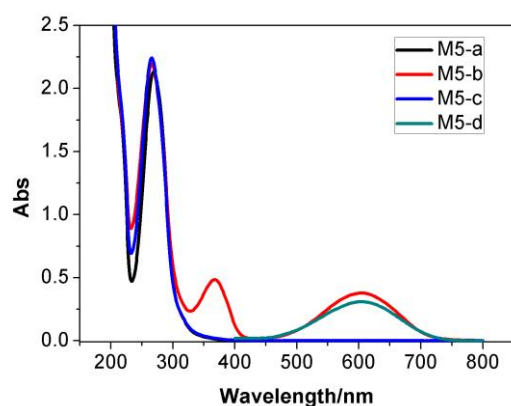
Figure S12 (a). Absorption spectra of **M3** (1.0×10^{-5} M) in acetonitrile (black curve), treated with potassium tert-butoxide (red curve), then neutralized with CH_3COOH (blue curve). Absorption spectrum of **M3** (1.0×10^{-3} M) in acetonitrile containing $TBAPF_6$ (0.1 M) under -3.0 V bias in ITO device (green curve).
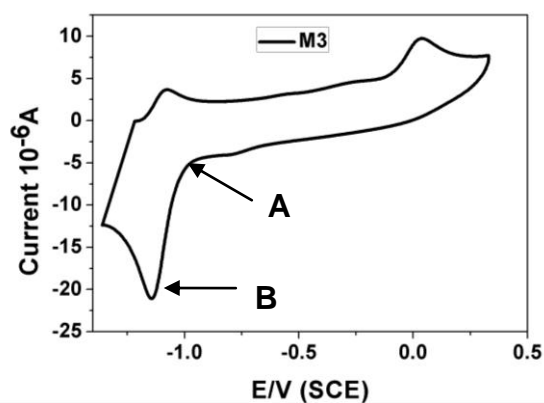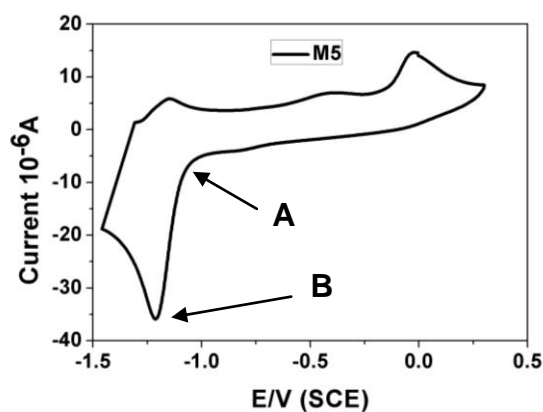

Figure S12 (b). Cyclic voltammogram (CV) of **M3** (1.0×10^{-3} M) in acetonitrile containing $TBAPF_6$ (0.1 M). Scan rate: 100 mV/s. The switch threshold of **M3** is labeled with arrow A and the oxidation peak of carbonyl group is labeled with arrow B.
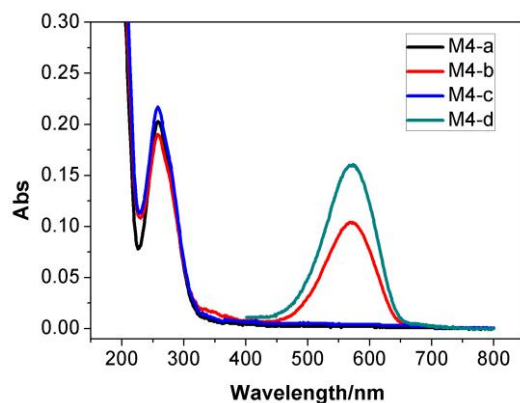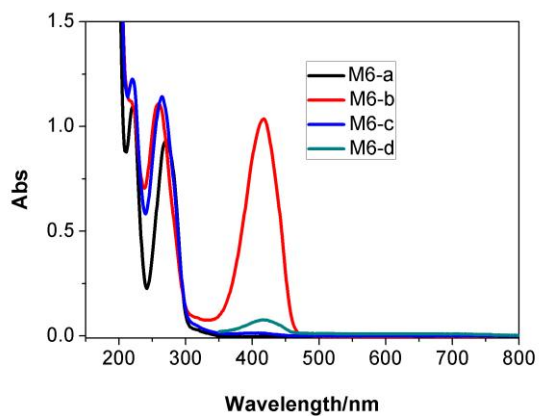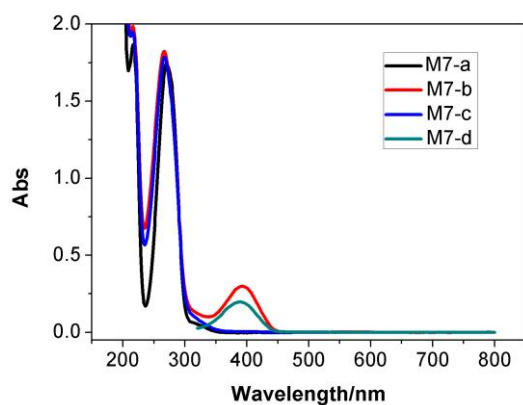
Figure S13 (a). Absorption spectra of **M4** (1.0×10^{-5} M) in acetonitrile (black curve), treated with potassium tert-butoxide (red curve), then neutralized with CH_3COOH (blue curve). Absorption spectrum of **M4** (1.0×10^{-3} M) in acetonitrile containing $TBAPF_6$ (0.1 M) under -3.0 V bias in ITO device (green curve).


Figure S13 (b). Cyclic voltammogram (CV) of **M4** (1.0×10^{-3} M) in acetonitrile containing $TBAPF_6$ (0.1 M). Scan rate: 100 mV/s. The switch threshold of **M4** is labeled with arrow A and the oxidation peak of carbonyl group is labeled with arrow B.

Figure S14 (a). Absorption spectra of **M5** (1.0×10^{-5} M) in acetonitrile (black curve), treated with potassium tert-butoxide (red curve), then neutralized with CH_3COOH (blue curve). Absorption spectrum of **M5** (1.0×10^{-3} M) in acetonitrile containing $TBAPF_6$ (0.1 M) under -3.0 V bias in ITO device (green curve).

Figure S14 (b). Cyclic voltammogram (CV) of **M5** (1.0×10^{-3} M) in acetonitrile containing $TBAPF_6$ (0.1 M). Scan rate: 100 mV/s. The switch threshold of **M5** is labeled with arrow A and the oxidation peak of carbonyl group is labeled with arrow B.

**Figure S15.** Absorption spectra of **M6** (1.0×10^{-5} M) in acetonitrile (black curve), treated with potassium tert-butoxide (red curve), then neutralized with CH_3COOH (blue curve). Absorption spectrum of mixture of **M6** (1.0×10^{-3} M) and nitrobenzene (1.0×10^{-3} M) in acetonitrile containing TBAPF$_6$ (0.1 M) under -3.0 V bias in ITO device (green curve).

Figure S16. Absorption spectra of **M7** (1.0×10^{-5} M) in acetonitrile (black curve), treated with potassium tert-butoxide (red curve), then neutralized with CH_3COOH (blue curve). Absorption spectrum of mixture of **M7** (1.0×10^{-3} M) and nitrobenzene (1.0×10^{-3} M) in acetonitrile containing $TBAPF_6$ (0.1 M) under -3.0 V bias (green curve).
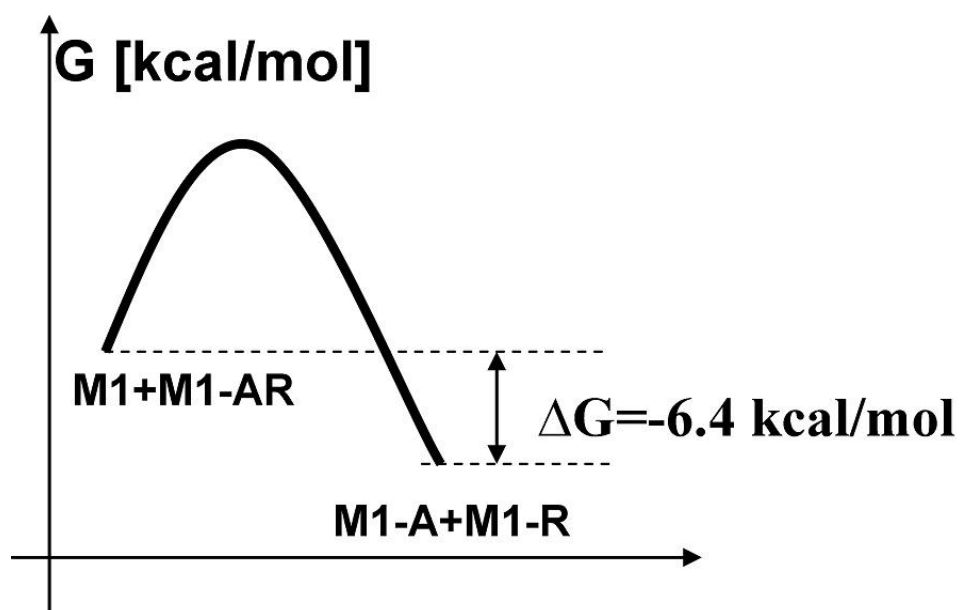
Figure S17. Schematic depiction of an adiabatic intermolecular proton transfer reaction. The free energy is plotted along the collective reaction coordinate, with the Gibb's free energy difference between reactant (**M1**:-820.4957 au; **M1-AR**: -820.5439 au) and product (**M1-A**: -819.9698 au; **M1-R**: -821.0801 au) denoted by ΔG. All the calculations were performed using the B3LYP/6-31+G(d,p).[1]
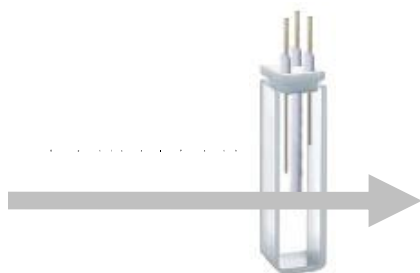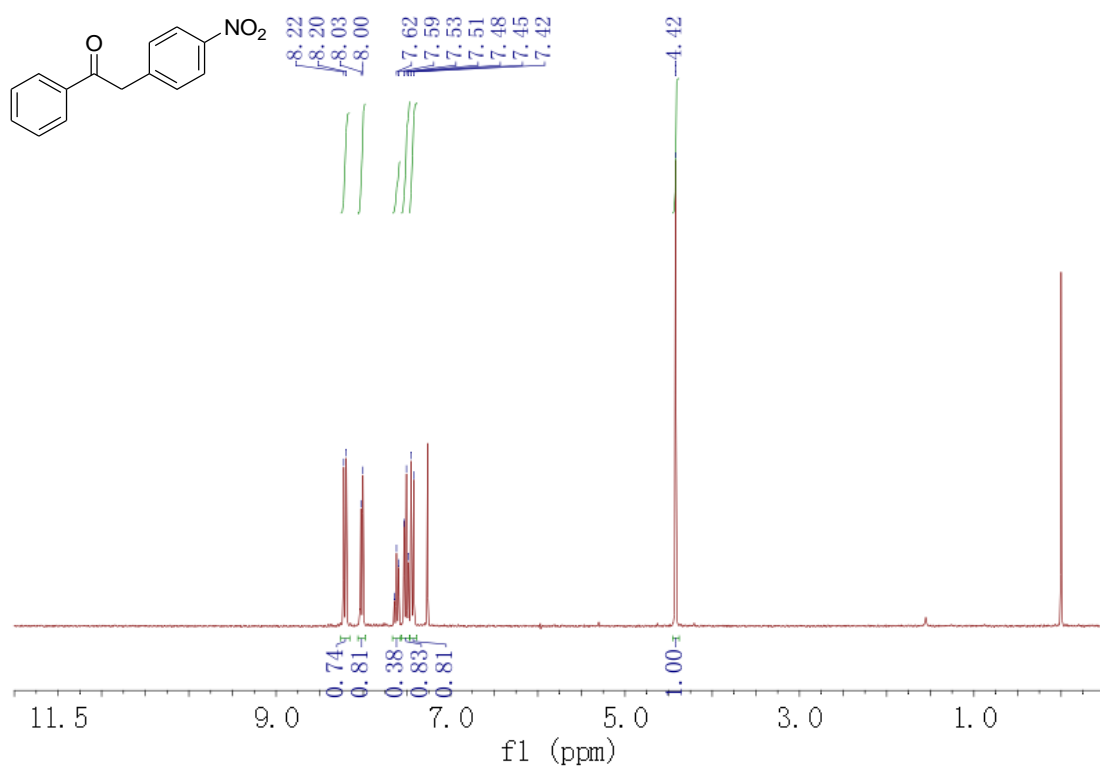
Figure S18. Illustration of in-situ Spectroelectrochemical Characterization
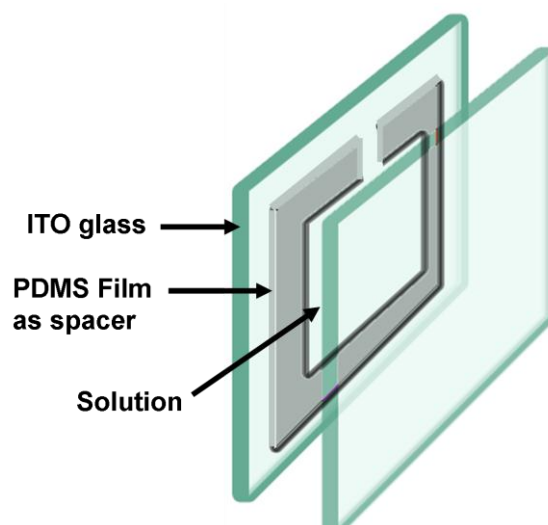
ITO glass

PDMS Film
as spacer

Solution

Figure S19. Illustration of the ITO cells of liquid film.

ITO glass
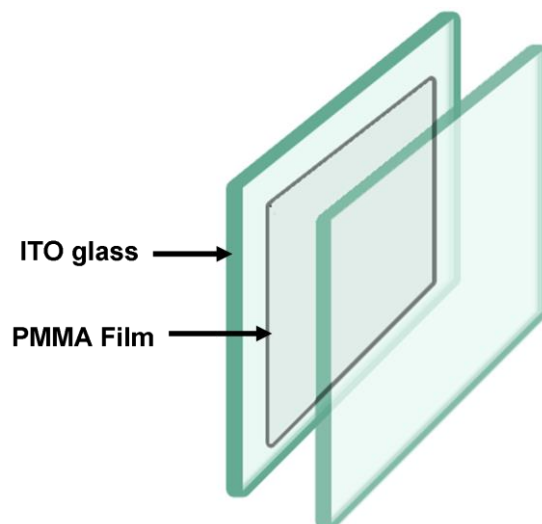
PMMA Film

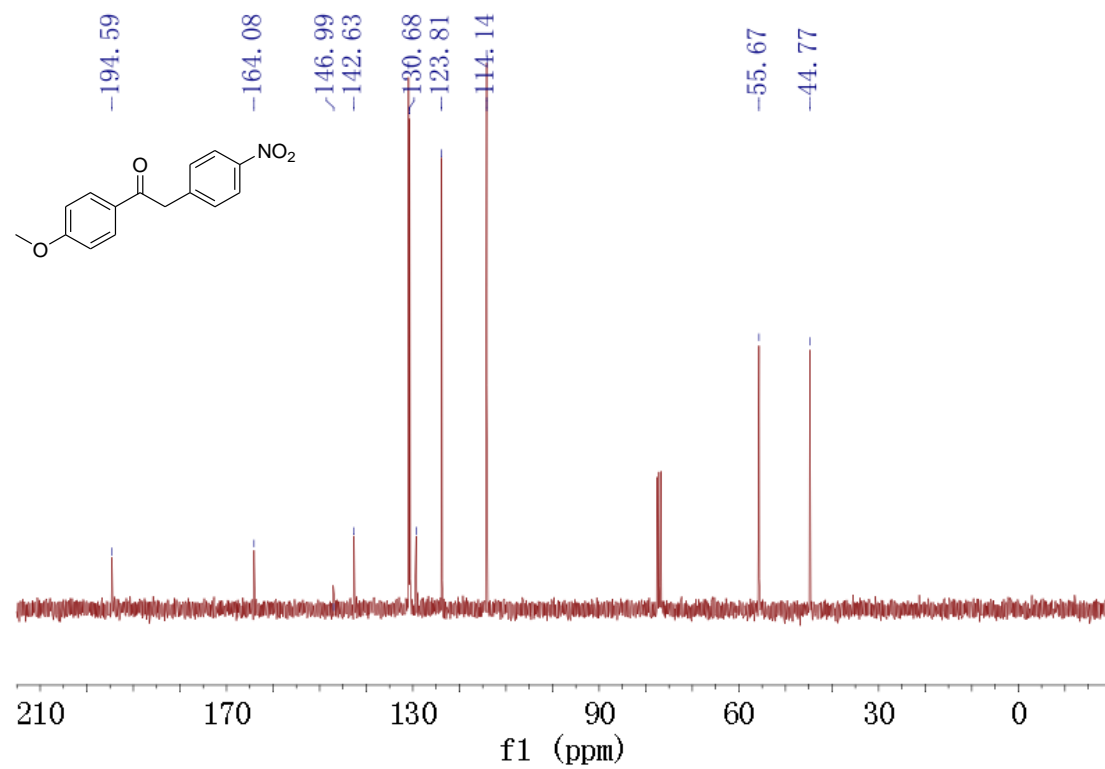**Figure S20.** Illustration of the ITO cells of PMMA film.

4. ^{1}H NMR and ^{13}C NMR of M1-M8

^{1}H NMR (300 MHz, CDCl$_3$) of **M1**
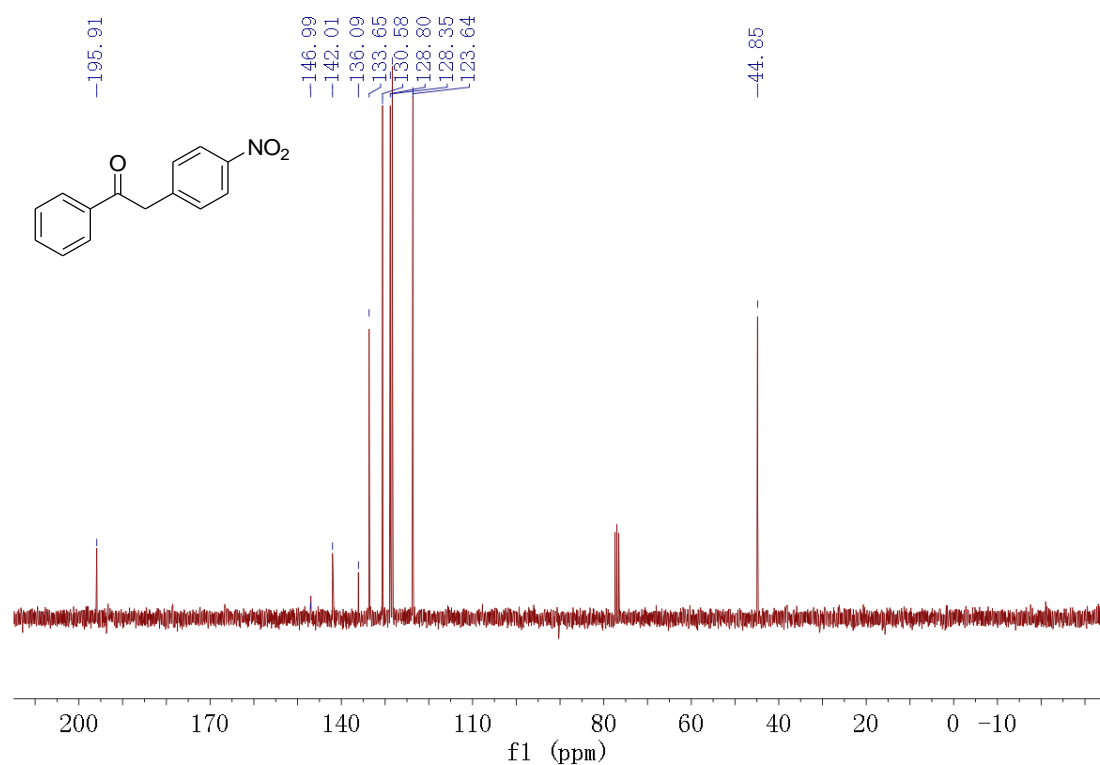
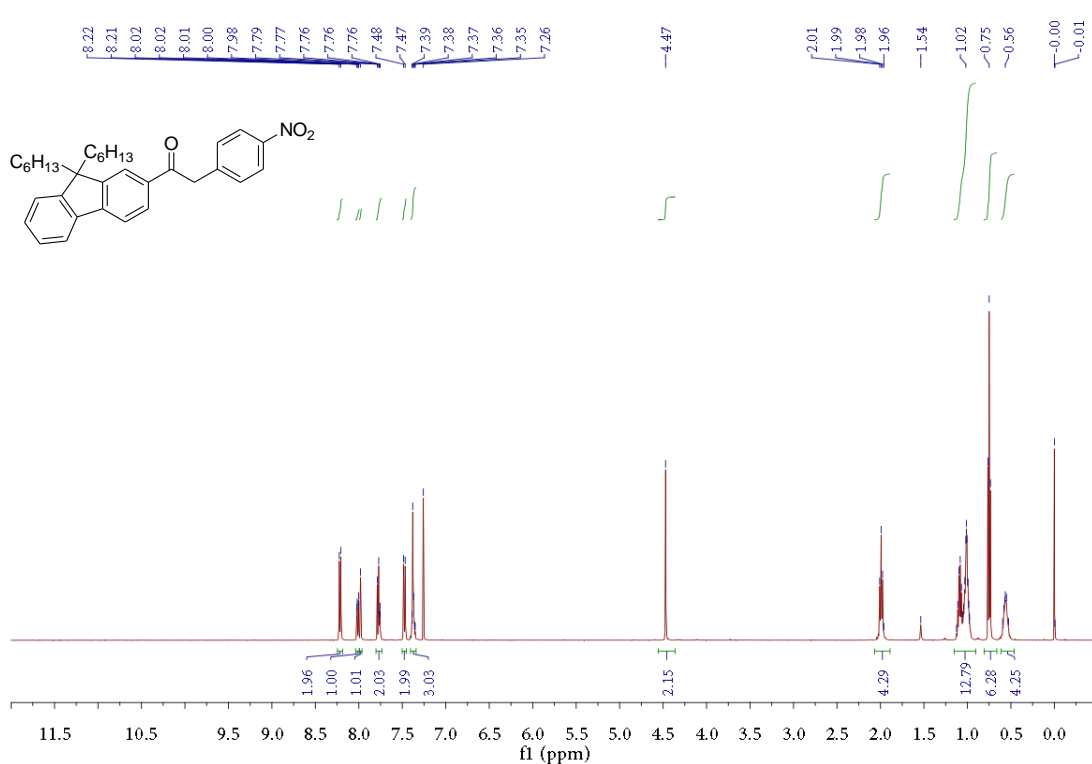^{13}C NMR (75 MHz, CDCl$_3$) of **M1**

^{1}H NMR (300 MHz, CDCl$_3$) of **M2**

^{13}C NMR (75 MHz, CDCl$_3$) of **M2**

^{1}H NMR (300 MHz, CDCl$_3$) of **M3**

^{13}C NMR (75 MHz, CDCl$_3$) of **M3**

^{1}H NMR (300 MHz, CDCl$_3$) of **M4**

^{13}C NMR (75 MHz, CDCl$_3$) of **M4**

^{1}H NMR (300 MHz CDCl$_3$) of **M5**

^{13}C NMR (75 MHz, CDCl$_3$) of **M5**

^{1}H NMR (300 MHz, CDCl$_3$) of **M6**

^{13}C NMR (75 MHz, CDCl$_3$) of **M6**

^{1}H NMR (300 MHz CDCl$_3$) of **M7**

^{13}C NMR (75 MHz, CDCl$_3$) of **M7**
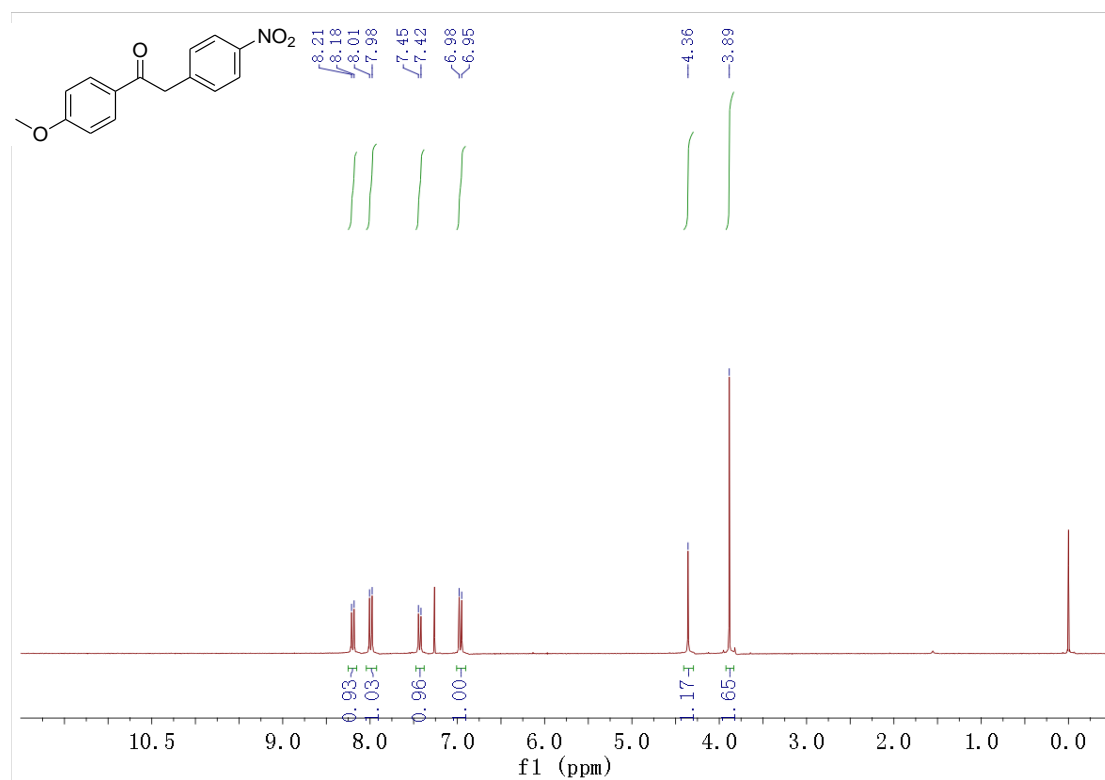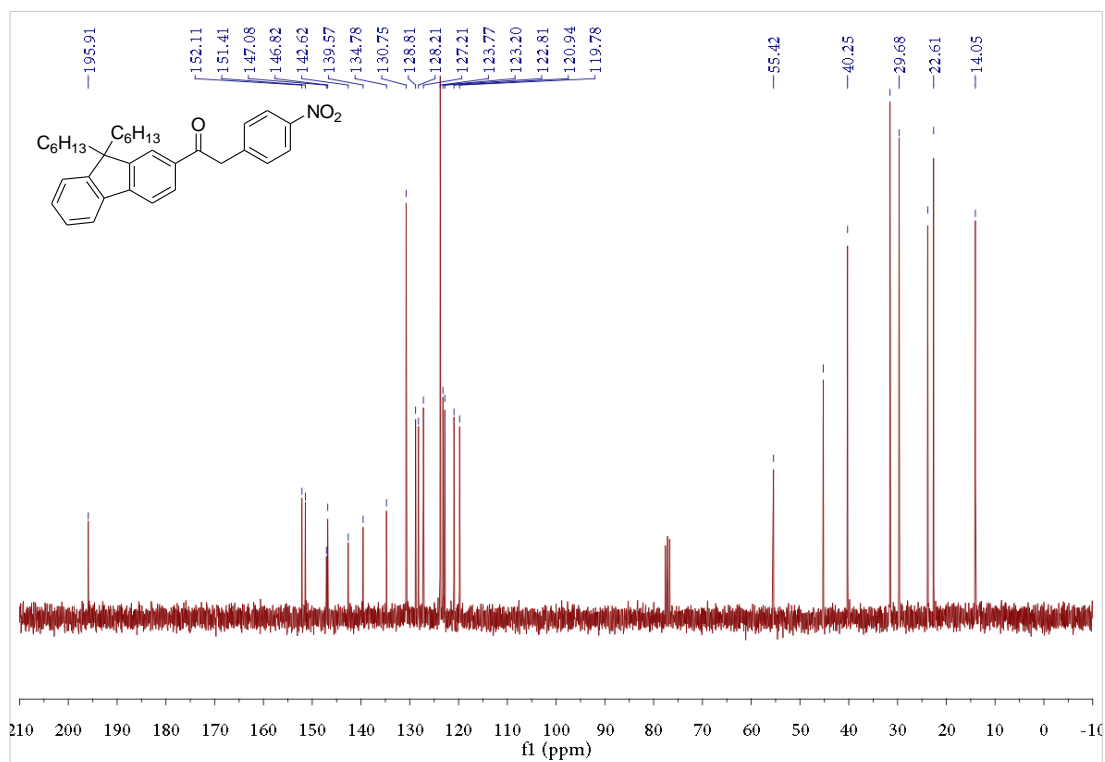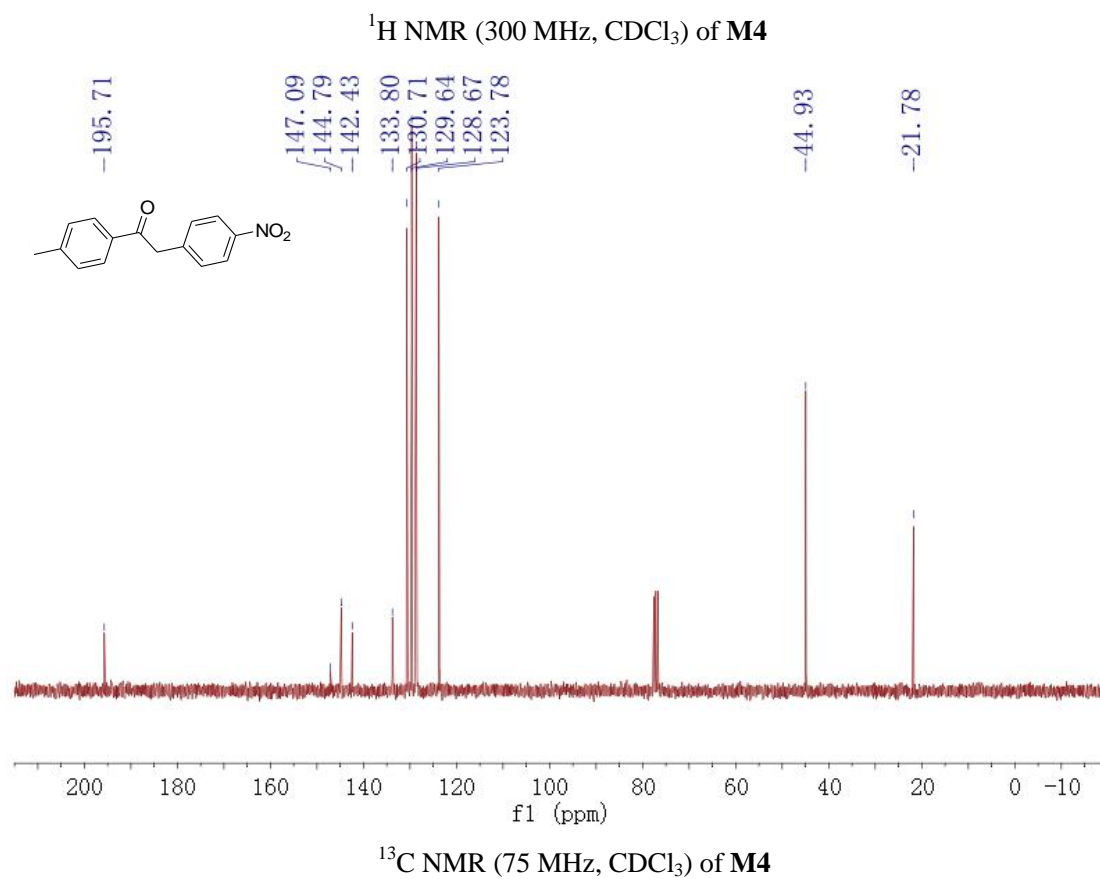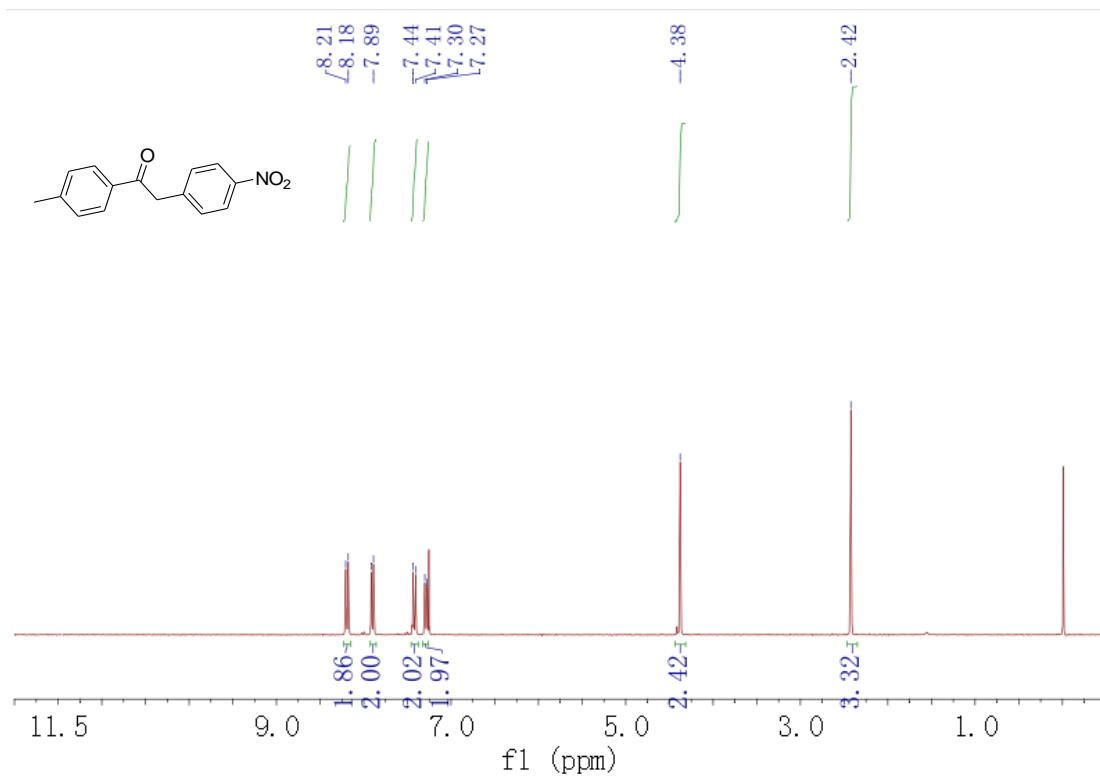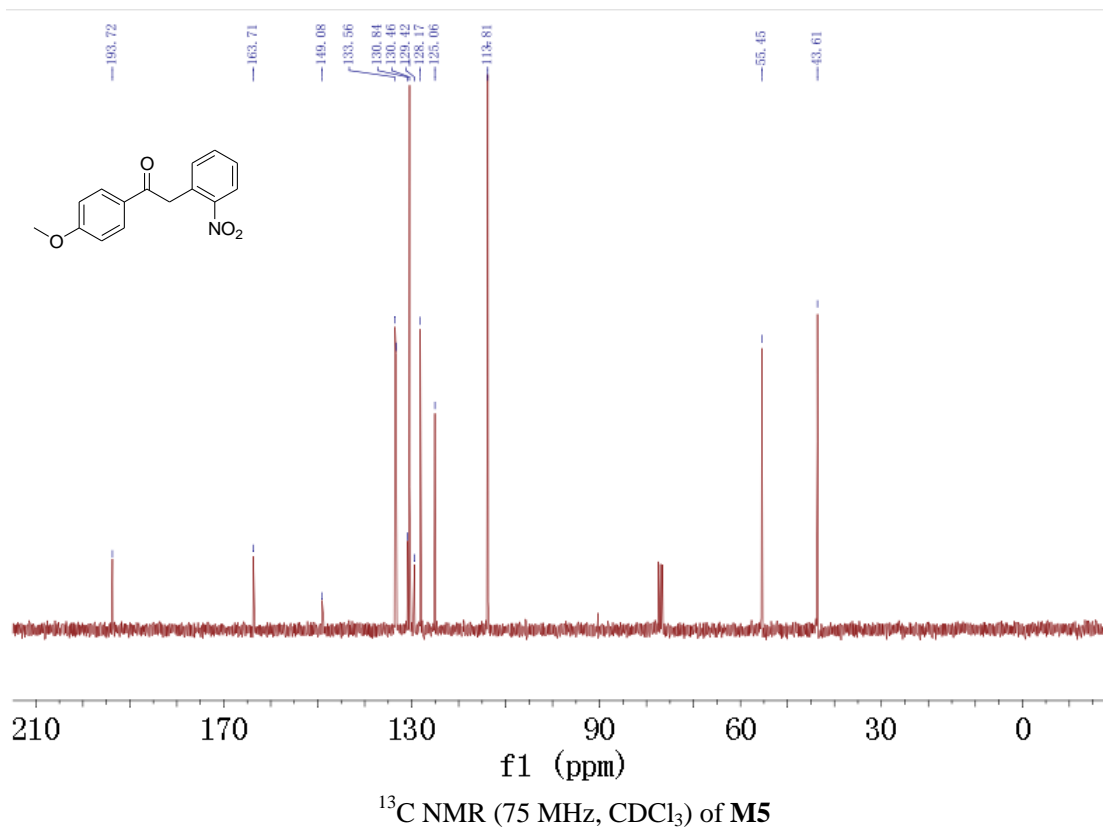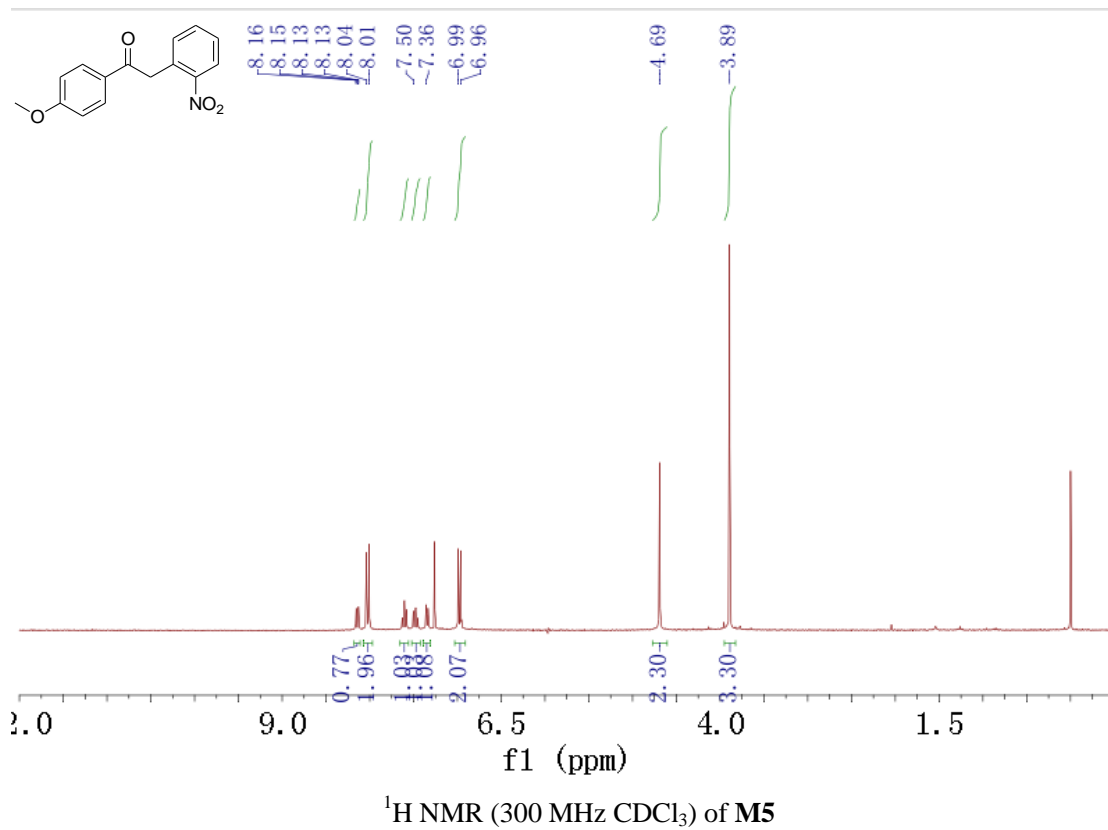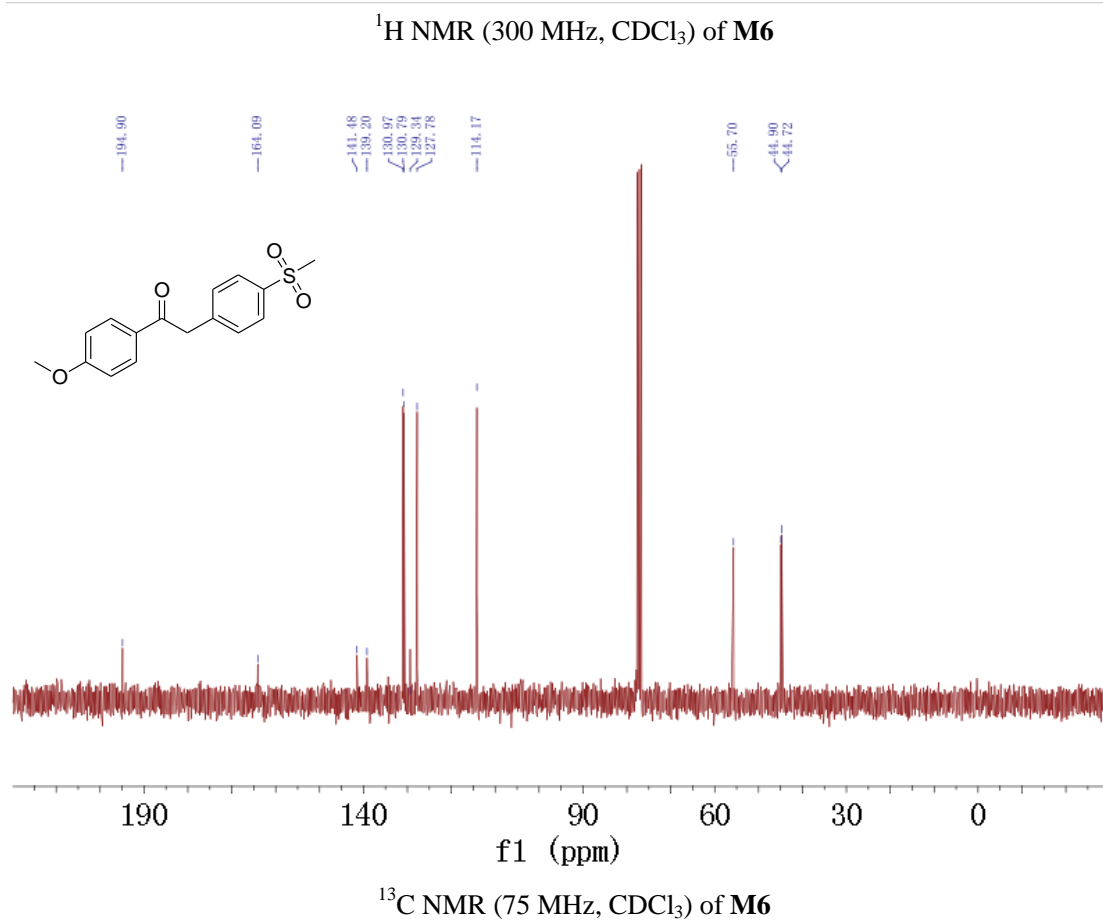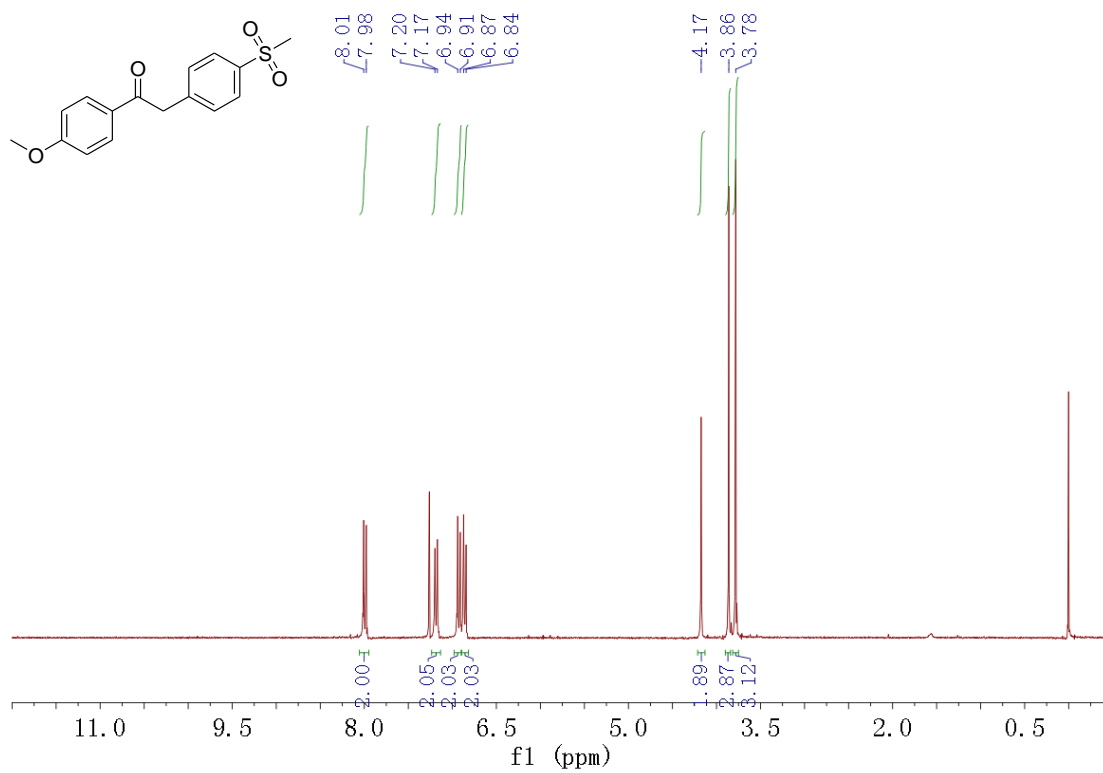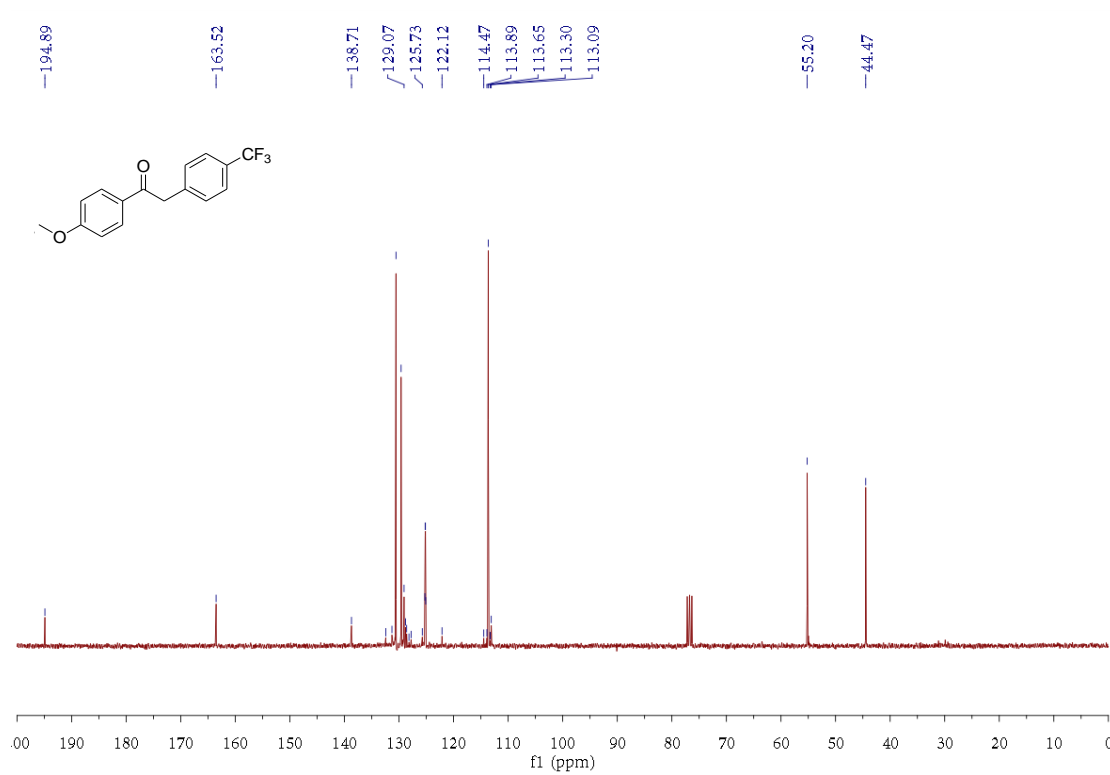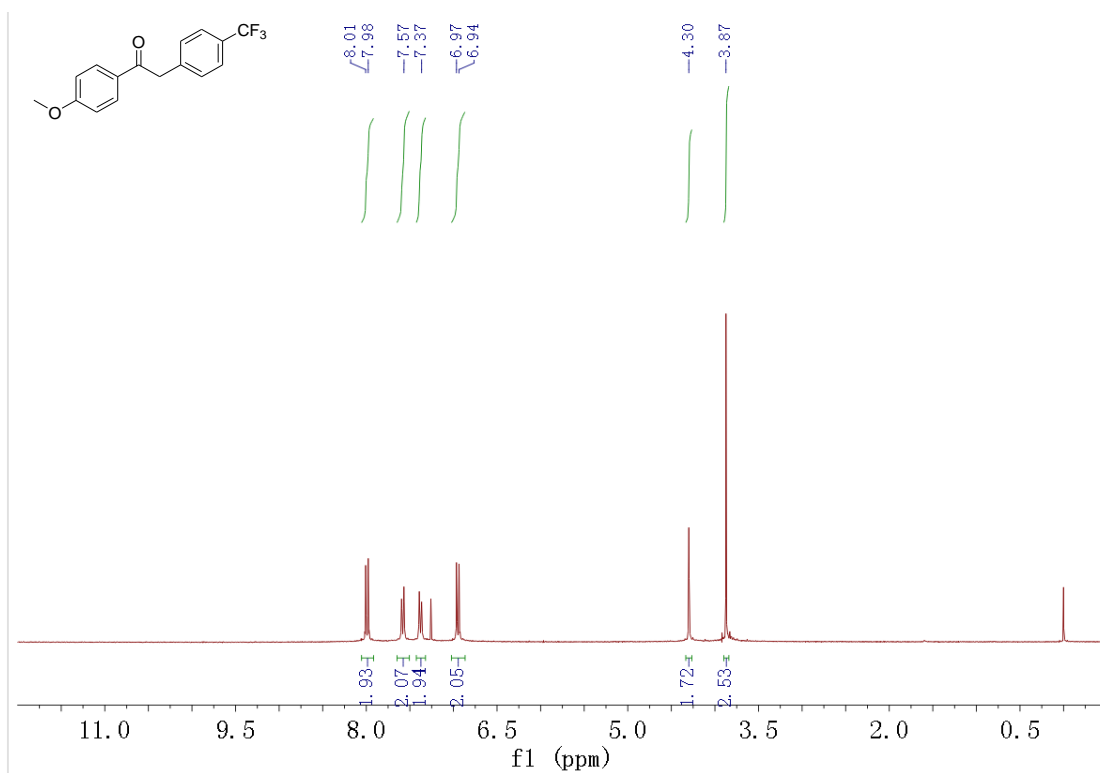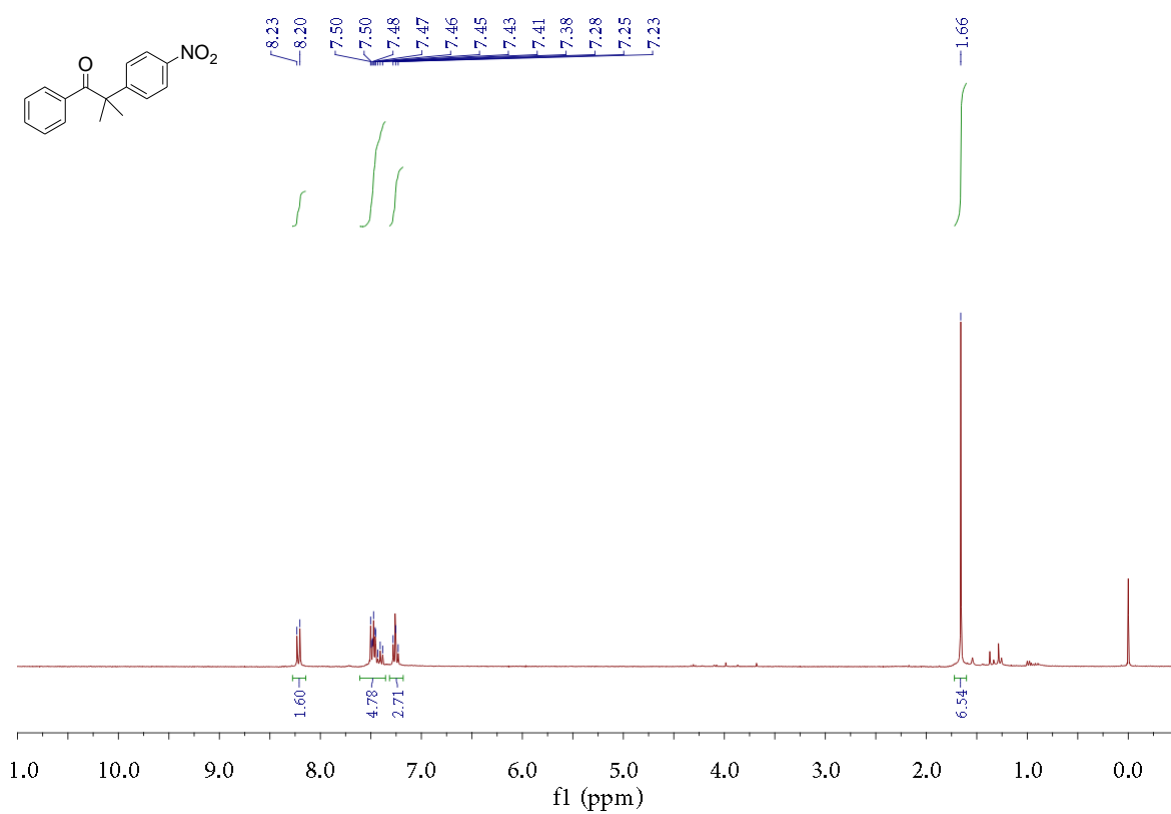
^{1}H NMR (300 MHz, CDCl$_3$) of **M9**

^{13}C NMR (75 MHz, CDCl$_3$) of **M9**

8.08
8.06
7.35
7.33
7.32
7.31
7.30
7.29
7.28
3.84
3.82
3.79
3.77
3.75
3.72
3.26

B (d)
8.07

D (m)
7.33

A (m)
3.79

C (s)
3.26

1.00
4.15
2.76
1.38

11.5 10.5 9.5 9.0 8.5 8.0 7.5 7.0 6.5 6.0 5.5 5.0 4.5 4.0 3.5 3.0 2.5 2.0 1.5 1.0 0.5 0.0
f1 (ppm)

^{1}H NMR (300 MHz, CDCl$_3$) of **M10**

146.48
143.51
141.46
131.36
127.89
127.85
125.38
122.48
109.08
64.46
46.48

200 190 180 170 160 150 140 130 120 110 100 90 80 70 60 50 40 30 20 10 0
f1 (ppm)

^{13}C NMR (75 MHz, CDCl$_3$) of **M10**
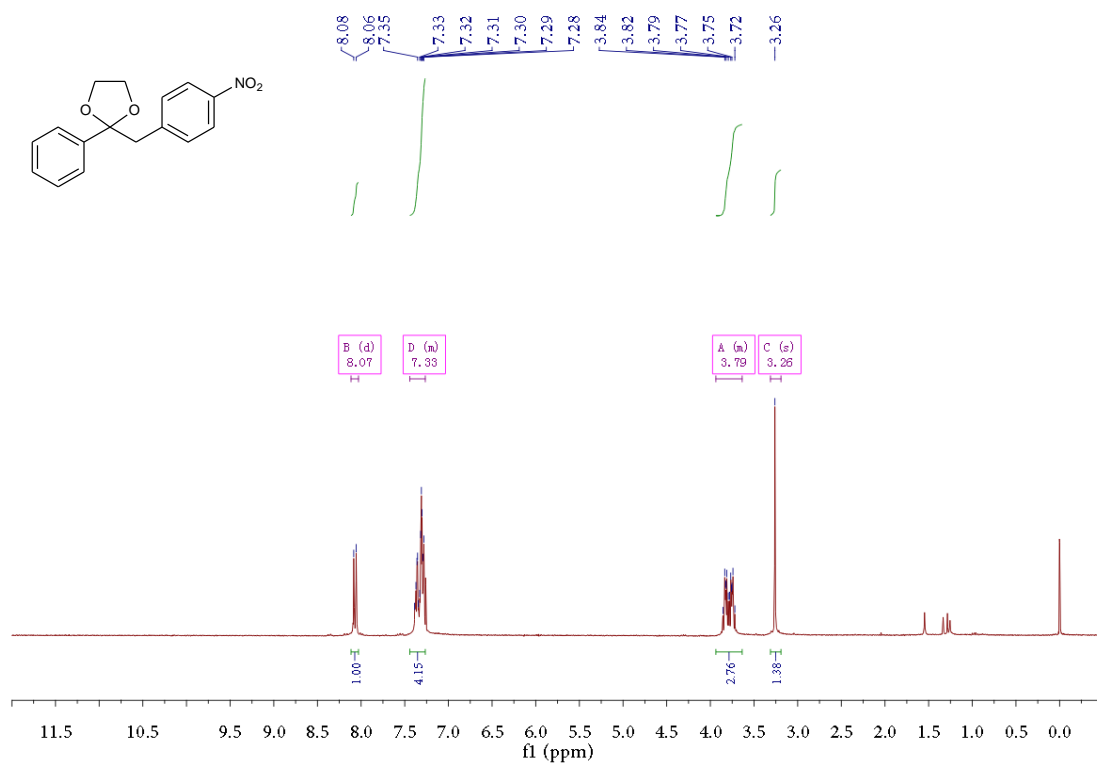
. ^{1}H NMR (300 MHz, CDCl$_3$) of **M11**
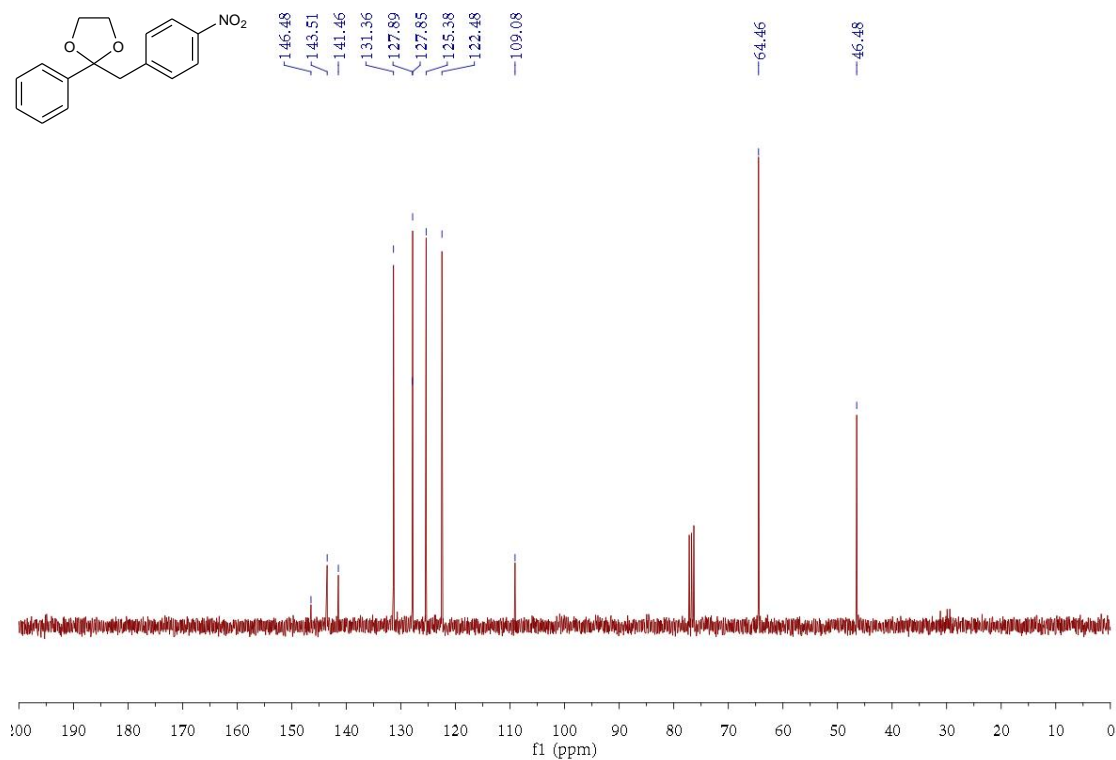
^{13}C NMR (75 MHz, CDCl$_3$) of **M11**
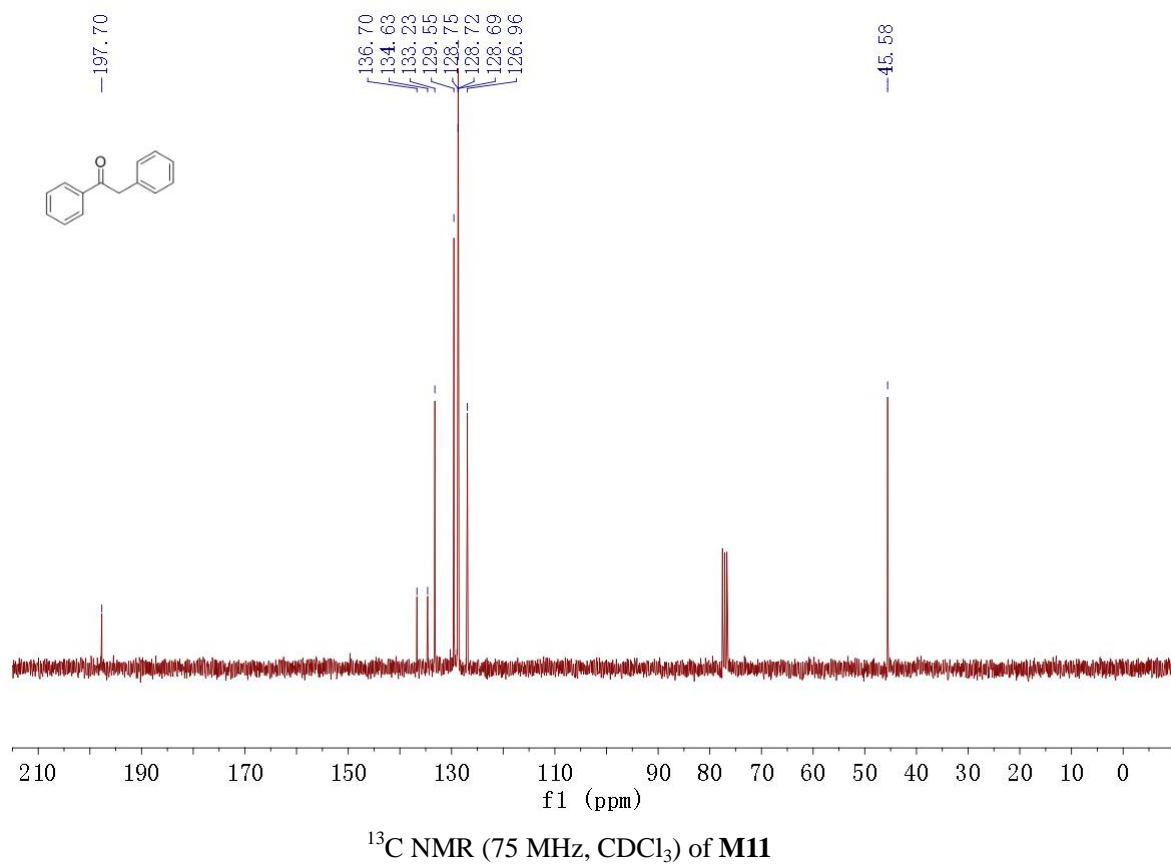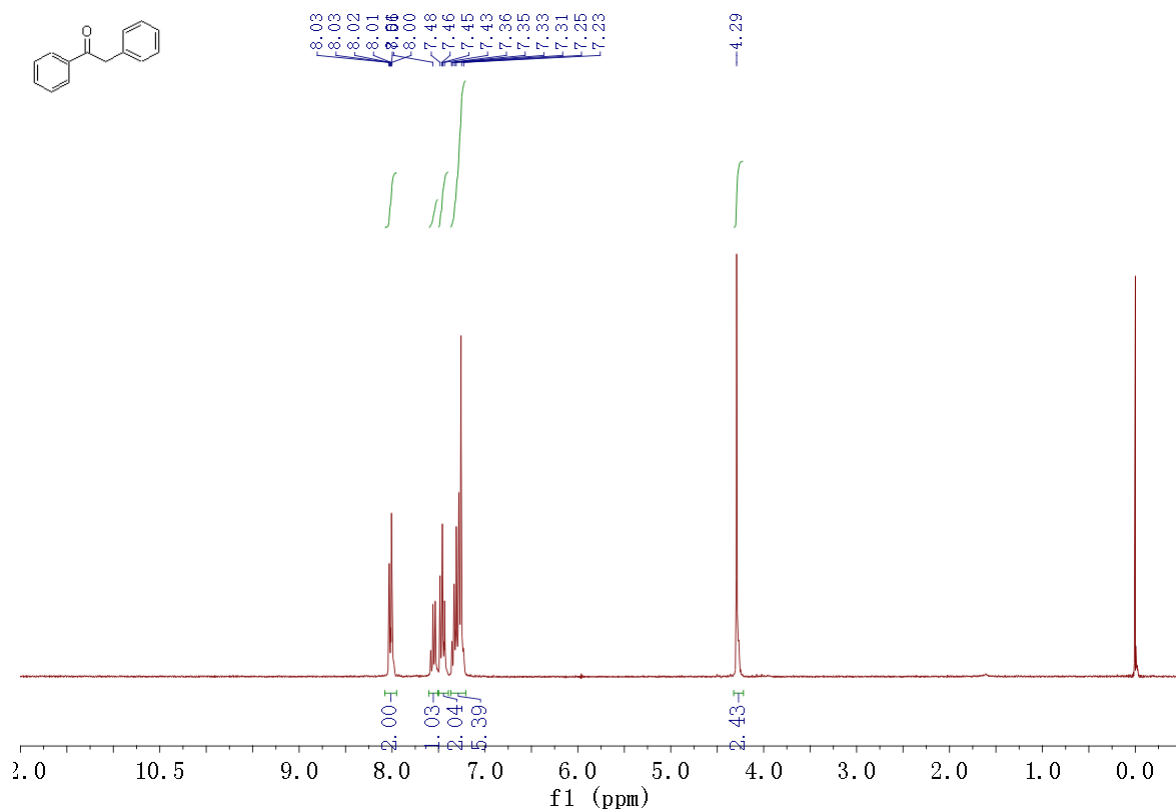
[1] M. J. Frisch, G. W. Trucks, H. B. Schlegel, G. E. Scuseria, M. A. Robb, J. R. Cheeseman, G. Scalmani, V. Barone, B. Mennucci, G. A. Petersson, H. Nakatsuji, M. Caricato, X. Li, H. P. Hratchian, A. F. Izmaylov, J. Bloino, G. Zheng, J. L. Sonnenberg, M. Hada, M. Ehara, K. Toyota, R. Fukuda, J. Hasegawa, M. Ishida, T. Nakajima, Y. Honda, O. Kitao, H. Nakai, T. Vreven, J. Montgomery, J. A. , J. E. Peralta, F. Ogliaro, M. Bearpark, J. J. Heyd, E. Brothers, K. N. Kudin, V. N. Staroverov, R. Kobayashi, J. Normand, K. Raghavachari, A. Rendell, J. C. Burant, S. S. Iyengar, J. Tomasi, M. Cossi, N. Rega, J. M. Millam, M. Klene, J. E. Knox, J. B. Cross, V. Bakken, C. Adamo, J. Jaramillo, R. Gomperts, R. E. Stratmann, O. Yazyev, A. J. Austin, R. Cammi, C. Pomelli, J. W. Ochterski, R. L. Martin, K. Morokuma, V. G. Zakrzewski, G. A. Voth, P. Salvador, J. J. Dannenberg, S. Dapprich, A. D. Daniels, O. Farkas, J. B. Foresman, J. V. Ortiz, J. Cioslowski, and D. J. Fox, *Gaussian 09, (Revision A. 02), Gaussian, Inc., Wallingford, CT* **2009**.